Cellular senescence and inflammation in aging and age-related disease

Wijshake, Tobias

CHAPTER 5

Phosphorylation of p65 at serine 467 is essential for proper transactivation of a subset of NF-κB target genes

Tobias Wijshake, Nicolette Huijkman, Henk van der Molen, Daphne Dekker, Niels Kloosterhuis, Darren Baker, Marten Hofker, Jan van Deursen, Lienhard Schmitz & Bart van de Sluis

In preparation

ABSTRACT

NF-κB is a key component of the inflammatory response, and constitutive NF-κB activation has been implicated in the development and progression of various disorders, including atherosclerosis, type 2 diabetes and cancer. Although, activation of the NF-κB pathway is well characterized, the exact mechanism by which nuclear NF-κB activity is accurately regulated remains ill defined. Recent studies have implicated an essential role for post-translational modifications of the activating subunit NF-κB p65 in the gene-specific activation and/or termination of transcription. To investigate the contribution of phosphorylation of p65 at serine 467 in murine NF-κB activity at the organismal level, we generated two knock-in mouse models carrying a mutation at residue 467 of *p65*. We replaced serine 467 with either an alanine or an aspartic acid, leading to non-phosphorylatable (S467A) or phospho-mimetic (S467D) mice, respectively. Here we report that homozygous S467A mice show diminished TNFα-induced expression of pro-inflammatory cytokines, while the expression of anti-apoptotic genes was not affected *in vivo*. This gene-specific regulation was confirmed in $p65^{S467A/S467A}$ mouse embryonic fibroblasts (MEFs). In contrast, mutation of serine 467 into aspartic acid results in increased transactivation of *Vcam1* and *Icam1* in MEFs. Taken together, these data demonstrate that phosphorylation of p65 at serine 467 is essential for selective induction of gene expression.

INTRODUCTION

The transcription factor NF-κB plays a critical role in the regulation of a vast amount of genes, including inflammatory cytokines, cell adhesion molecules and anti-apoptotic genes. Hereby NF-κB controls many biological processes, such as inflammation, cell survival, proliferation and differentiation [1,2]. In an inactive state, NF-κB associates with inhibitory IκB proteins, which results in the sequestration of these complexes in the cytoplasm [1]. NF-κB activation via the canonical pathway is facilitated by the upstream IκB kinase (IKK), which consists of two catalytically active kinases, IKKα and IKKβ, and a regulator subunit known as NF-κB essential modulator (NEMO) [1]. Upon stimulation, the activated IKK complex phosphorylates IκBα at two N-terminal serine residues. Phosphorylated IκBα is subsequently polyubiquitinated and undergoes proteasomal degradation, which enables the translocation of canonical NF-κB subunits p65 and p50 to the nucleus, where it can bind to cognate κB-sequences and activate transcription of numerous genes [2,3].

Sustained NF-κB activity has been implicated in a large variety of diseases, including inflammatory, metabolic, and immunological disorders, cancer, aging, and age-related diseases [4-7], indicating the necessity of specific and accurate termination of NF-κB-mediated transcription. Recent studies have demonstrated that the NF-κB transactivating subunit p65 undergoes multiple post-translational modifications, including phosphorylation, acetylation, methylation and ubiquitination, that are essential for the intensity and duration of nuclear NF-κB activity and the control of the exact transcriptional output [8,9]. These post-translational modifications can occur at multiple sites of p65, and numerous phosphorylation sites have been implicated in either increased or decreased NF-κB-mediated transcription depending on the stimulus, the phosphorylation site and the target genes [8].

Phosphorylation of p65 at serine 276 increases NF-κB transcriptional activity in response to various stimuli, probably through a conformational change that results in enhanced or decreased binding of co-factors [8,10,11]. Knock-in mice in which serine 276 was replaced by an aspartic acid (S276D) showed a progressive, systemic hyperinflammatory condition resulting in severe runting and eventually death between postnatal days 8-20 [12]. In contrast, knock-in embryos expressing a p65 mutant carrying an alanine instead of a serine at position 276 (S276A) die at different embryonic days due to a number of variegated developmental anomalies, which were caused by epigenetic repression [13]. Along this line, phosphorylation at threonine 505 was demonstrated to be a negative regulator of various biological processes, including apoptosis, autophagy, proliferation, and migration *in vitro* [14].

Phosphorylation of p65 at serine 468 is mediated by various kinases such as glycogen synthase kinase 3 beta (GSK-3β), IKKβ, and IKKε [15-17]. It has been demonstrated that phosphorylation of p65 at serine 468 contributes to the selective termination of NF-κB dependent gene expression [18]. TNF-induced phosphorylation of p65 serine 468 is essential for the binding of an ubiquitin ligase complex, which includes the components COMMD1 and cullin 2. This multimeric ubiquitin ligase complex mediates ubiquitination and proteasomal-dependent removal of chromatin-bound p65 at promoter sites of a subset of NF-κB genes [18,19]. Analysis of NF-κB target gene expression in MEFs expressing a non-phosphorylatable form of p65 (S468A) confirmed that regulation of transcription at serine 468 is highly target gene-specific [16,18,20]. However, genetic evidence that assesses the importance of phosphorylation at p65 serine 468 at the molecular, cellular and organismal level is still lacking. To address this, we generated two knock-in mouse models expressing a

p65 serine 467 mutant (corresponding to human p65 serine 468). We substituted serine 467 with either an alanine or an aspartic acid, resulting in *p65*^{S467A} ("non-phosphorylatable") or *p65*^{S467D} ("phospho-mimetic") mice, respectively. We demonstrated that mice expressing the p65 S467A mutant have impaired TNFα-induced transactivation of pro-inflammatory genes. In addition, MEFs derived from *p65*$^{S467A/S467A}$ mice have diminished total p65 protein levels, showed impaired TNF-induced expression of NF-κB-mediated genes, and decreased cell viability. In contrast to previous *in vitro* studies, here we demonstrate that phosphorylation of murine p65 at serine 467 is crucial for the transactivation of a subset of NF-κB target genes.

RESULTS

Generation of *p65* S467A knock-in mice

To assess the biological importance of phosphorylation at p65 serine 467 (corresponding to human p65 serine 468), we generated a knock-in mouse in which serine 467 is substituted by an alanine ("non-phosphorylatable"). Using homologous recombination in embryonic stem (ES) cells, we replaced the thymine with a guanine in the murine *p65* gene at position c.1399, resulting in the substitution of alanine for serine (S467A) (Figure 1A). We obtained chimeric mice by microinjection of correctly targeted ES clones into C57BL6/J blastocysts. These

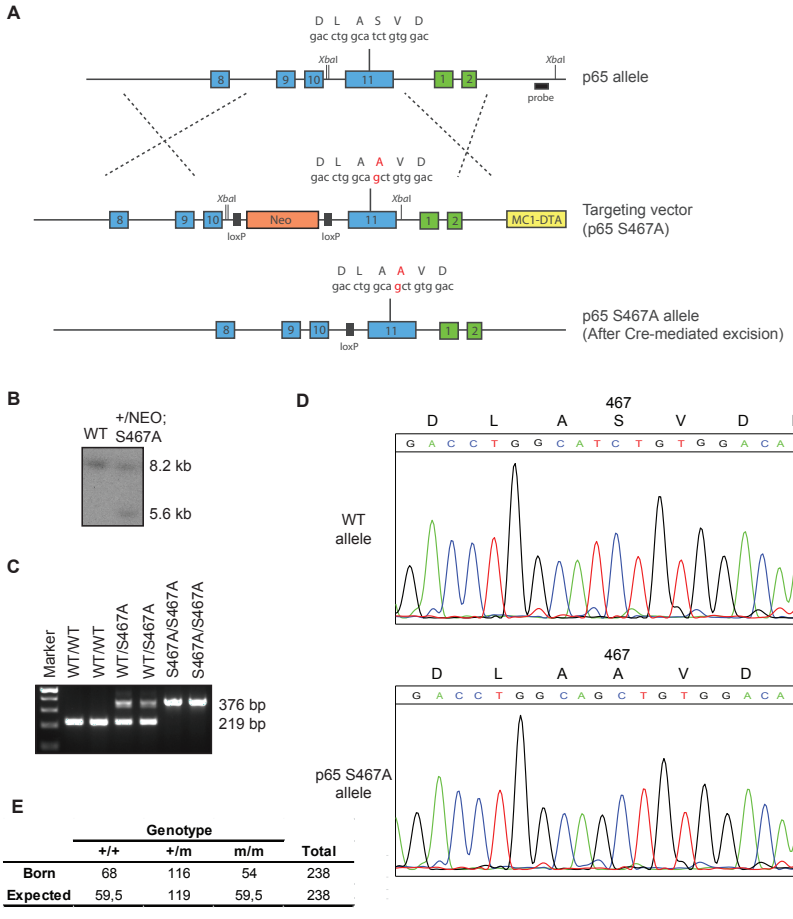

	Genotype			
	+/+	+/m	m/m	Total
Born	68	116	54	238
Expected	59,5	119	59,5	238

Figure 1. Serine to alanine substitution at residue 467 of *p65*. (A) Gene targeting strategy to generate $p65^{S467A/S467A}$ mice. Indicated are the genomic mouse *p65* locus spanning exon 8-11 of *p65* and exon 1-2 of *Sipa1* (top); the targeting vector with the T>G substitution in exon 11 (red), loxP sites (black boxes); the p65 S467A locus after targeted recombination and crossing with *Hprt*-Cre recombinase mice to remove the NEO cassette and produce $p65^{+/S467A}$ mice. **(B)** Southern blot of *Xba*I digested genomic DNA from two ES cell clones and probed with DNA fragment showing the 8.2 kb and 5.6 kb fragments representing the wild-type and $p65^{NEO;S467A}$ allele, respectively. **(C)** PCR genotyping of DNA extracted from the tails of two wild-type, two $p65^{+/S467A}$ and two $p65^{S467A/S467A}$ mice. **(D)** Sequencing of p65 cDNA obtained by RT-PCR from livers of wild-type and $p65^{S467A/S467A}$ mice. **(E)** Genotype analysis of offspring derived from breeding S467A heterozygous parents. The expected Mendelian frequency is indicated at the bottom.

chimeras successfully transmitted the mutated *p65* allele (referred to as $p65^{NEO;S467A}$) to their offspring (Figure 1B). $p65^{+/NEO;S467A}$ mice were crossed with *Hprt*-Cre transgenic mice [21] to excise the NEO gene cassette (Figure 1A). Genotyping of genomic DNA from pups derived from breeding of heterozygous $p65^{+/S467A}$ mice resulted in the generation of $p65^{S467A/S467A}$ mice (Figure 1C). Sequencing the p65 cDNA of wild-type and $p65^{S467A/S467A}$ mice confirmed the replacement of thymine into a guanine at position c.1399 (Figure 1D). Homozygous knock-in ($p65^{S467A/S467A}$) mice were obtained at the expected Mendelian frequency and were overtly indistinguishable from control littermates in their first year of life (Figure 1E).

S467A mutation results in reduced p65 protein levels

To address the role of p65 phosphorylation at serine 467 in regulating NF-κB-mediated transcription, we cultured MEFs from wild-type and $p65^{S467A/S467A}$ littermates derived from 13.5 dpc embryos. Western blot analysis of wild-type and homozygous knock-in fibroblast lysates demonstrated that $p65^{S467A/S467A}$ MEFs have a significantly reduced amount of p65 protein. Quantitation of p65 signal revealed that homozygous knock-in fibroblasts have p65 protein levels of ~30% compared to $p65^{+/+}$ MEFs (Figure 2A). To assess whether this reduction is due to decreased transcription of the mutated *p65* allele, we determined the *p65* mRNA levels in both wild-type and $p65^{S467A/S467A}$ MEFs by qRT-PCR. Levels of *p65* mRNA was unaltered in homozygous knock-in fibroblasts compared to wild-type cells, indicating that the reduced p65 protein level was not caused by impaired gene transcription (Figure 2A). Western blot analysis of various tissue homogenates showed a clear reduction in p65 protein levels in lung and gastrocnemius muscle of $p65^{S467A/S467A}$ mice compared to wild-type controls (Supplemental Figure 1). The difference in the p65 protein was less clear in liver, kidney and heart tissue of wild-type and $p65^{S467A/S467A}$ mice, but is still trending towards a reduction in homozygous knock-in mice (Supplemental Figure 1). A possible explanation for the reduced p65 protein levels might be that the mutated p65 protein results in conformational changes which makes the protein unstable and subject to rapid proteasomal degradation [22].

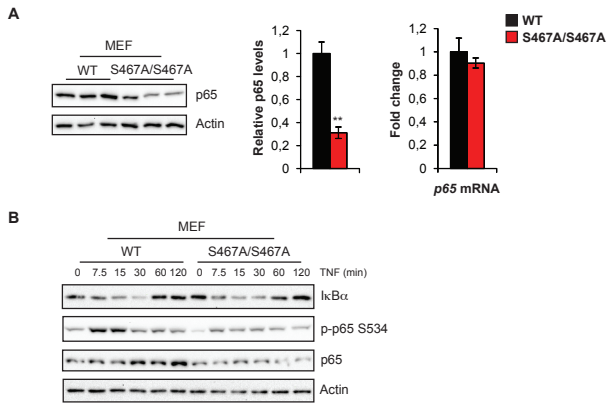

Figure 2. Characterization of *p65* S467A mutant MEFs. (A) Immunoblot analysis of p65 protein levels in wild-type and S467A MEFs generated from embryos at 13.5 dpc. Actin was used as a loading control (left). Quantitation of relative p65 protein amount in 3 independent wild-type and homozygous knock-in MEF lines shown on left (middle). Relative *p65* mRNA expression of wild-type and homozygous knock-in MEFs as determined by quantitative RT-PCR (right). All values represent average ± SEM, ** = $P < 0.01$. **(B)** Western blot analysis of degradation and resynthesis of IκBα proteins in whole cell extracts of MEFs after TNFα stimulation (10ng/ml). In addition, the levels of phosphorylated p65 at serine 534 in wild-type and $p65^{S467A/S467A}$ MEFs are indicated.

Next, we determined whether the upstream NF-κB activation in S467A MEFs was affected. Time course analysis of TNFα-mediated NF-κB activation demonstrated normal kinetics of IκBα degradation and resynthesis in homozygous knock-in fibroblasts (Figure

2B). Furthermore, TNFα-mediated phosphorylation of p65 at serine 534 (corresponding to human p65 serine 536) showed similar kinetics in both wild-type and *p65*$^{S467A/S467A}$ MEFs. Although, the amount of phosphorylated p65 and total p65 was less in the homozygous knock-in fibroblasts (Figure 2B). Altogether, these data demonstrate that mutation of serine 467 to alanine results in decreased p65 levels in MEFs and in various tissues, but it does not affect the upstream activation of the NF-κB pathway.

Absent phosphorylation at serine 467 impairs transactivation of NF-κB-dependent genes

Previous studies have demonstrated that phosphorylation of p65 has an essential role in the transcriptional output of NF-κB [12,13,16-18,20]. To determine whether the S467A mutation affects NF-κB-mediated transcription, we examined the inducible expression of a number of well-known NF-κB target genes. We stimulated both wild-type and *p65*$^{S467A/S467A}$ MEFs with TNFα and monitored the expression kinetics of these genes by qRT-PCR. Homozygous knock-in MEFs showed impaired transactivation of various pro-inflammatory cytokines, including *Tnfα, Il-1α*, and *Mcp-1* (Figure 3A). In addition, the gene expression of two cell adhesion molecules, namely *Icam1* and *Vcam1* was markedly reduced in S467A mutant MEFs (Figure 3A). Moreover, the transactivation of a number of anti-apoptotic genes was

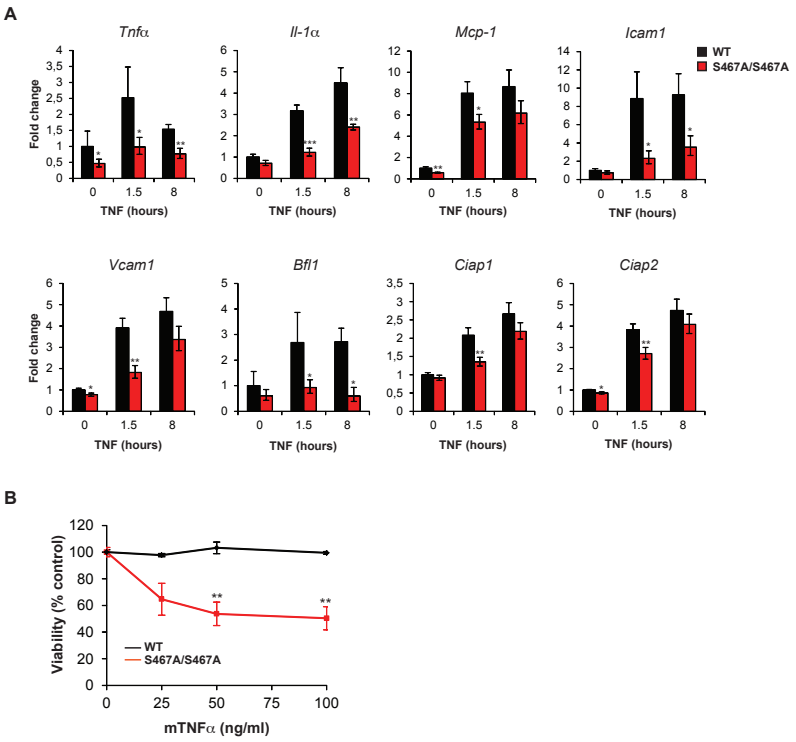

Figure 3. Impaired activation of NF-κB-mediated gene expression. (A) Relative mRNA expression of pro-inflammatory cytokines, NF-κB target genes and anti-apoptotic genes at 0, 1,5 and 8 hours after TNFα stimulation (10ng/ml). Values represent 6 independent wild-type and S467A MEF lines. **(B)** Cell viability was assessed in wild-type and S467A MEFs after 24-hours exposure to various amounts of TNFα. We used 3 independent MEF lines. All values represent average ± SEM, * = $P < 0.05$, ** = $P < 0.01$, and *** = $P < 0.001$.

impaired in homozygous knock-in fibroblasts (Figure 3A). In contrast, expression of several additional NF-κB target genes, such as *IκBα*, *Il-6* and *A20* were not markedly changed in *p65*$^{S467A/S467A}$ MEFs (Supplemental Figure 2). Taken together, the above data demonstrate that loss of phosphorylation at serine 467 impairs the transactivation of a subset of NF-κB target genes.

As substitution of serine 467 by an alanine impaired the transactivation of various anti-apoptotic genes (Figure 3A), we decided to examine if homozygous S467A MEFs are sensitive to TNFα-induced cell death. Cell viability assays in which we exposed MEFs to various concentrations of TNFα resulted in reduced cell viability in mutant S467A MEFs, while wild-type MEFs were unaffected (Figure 3B).

To investigate whether the impaired activation of NF-κB target genes and reduced cell viability in *p65*$^{S467A/S467A}$ MEFs is due to reduced p65 protein levels, we repeated these analyses in *p65*$^{+/-}$ MEFs. Western blot analysis in *p65*$^{+/-}$, *p65*$^{-/-}$ and *p65*$^{S467A/S467A}$ cells demonstrated that total p65 protein levels were ~55%, 0% and ~30%, respectively of those in *p65*$^{+/+}$ MEFs (Supplemental Figure 3A). Basal and TNFα-induced expression of several pro-inflammatory, anti-apoptotic and other NF-κB target genes showed a two-fold reduction in *p65*$^{+/-}$ MEFs compared to control cells (Supplemental Figure 3B). This suggests that reduced p65 protein levels in *p65*$^{S467A/S467A}$ MEFs can not completely account for the differential impairment in TNFα-induced NF-κB transactivation (Figure 3 and Supplemental Figure 2). Next, we repeated the cell viability assay and similar to our previous experiment (Figure 3B), homozygous knock-in cells showed a significant reduction in cell viability (Supplemental Figure 3C). Despite the reduced expression of anti-apoptotic genes, *p65* haplo-insufficient MEFs demonstrated no increased sensitivity to TNF-induced cell death compared to wild-type controls (Supplemental Figure 3B-C). Taken together, these data suggest that diminished p65 protein levels in *p65*$^{S467A/S467A}$ MEFs cannot completely explain the observed differences in TNFα-induced NF-κB transactivation and cell viability.

Gene-specific regulation of NF-κB target genes in S467A mutant mice

Genetic inactivation of hepatic *p65* sensitizes mice to lethal liver injury upon TNF administration. In depth analysis demonstrated a huge increase in transaminase levels and liver apoptosis in liver-specific *p65* knockout mice [23]. This combined with the observed TNFα-induced cell death in the S467A MEFs, prompted us to test whether *p65*$^{S467A/S467A}$ mice are sensitive to liver induced injury upon TNFα administration. However, examination of transaminase concentrations at 12 hours after orbital TNFα injection (15μg/kg) showed no detectable enhancement of ALT/AST plasma levels in both wild-type and homozygous knock-in mice, indicating that *p65*$^{S467A/S467A}$ mice have no increased sensitivity to TNFα-induced liver injury (data not shown).

Next, we evaluated whether the S467A mutation affects the activation of NF-κB *in vivo*. Wild-type and S467A mutant mice received an injection with either PBS or TNFα (15μg/kg) and the expression of various NF-κB genes by qRT-PCR was examined. Analysis of a number of tissues at 1 hour post injection revealed that *Icam1* expression was markedly reduced in liver, kidney, heart, lung and gastrocnemius muscle of *p65*$^{S467A/S467A}$ mice (Figure 4). Furthermore, the induced expression of inflammatory cytokines, including *Mcp1, Tnfα,* and *Il-6* was impaired in most tissues of S467A mutant mice (Figure 4). In contrast, activation of anti-apoptotic gene expression was not affected in *p65*$^{S467A/S467A}$ mice (Supplemental Figure 4), indicating that serine 467 of p65 is implicated in the gene-specific regulation of NF-κB target genes *in vivo*.

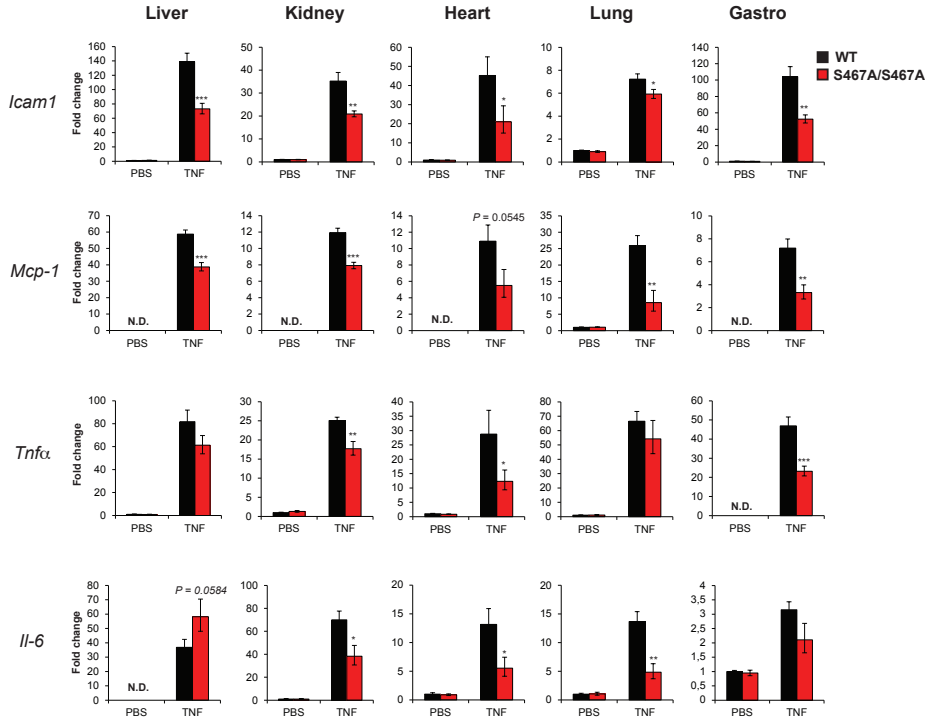

Figure 4. Gene-specific regulation of inflammation. Expression of pro-inflammatory and NF-κB target genes was assessed in various tissues at 1 hour after orbita injection with either PBS or TNFα (15μg/kg). PBS, n = 7 male mice per genotype; TNFα, n = 6 male mice per genotype. All values represent average ± SEM, * = $P < 0.05$, ** = $P < 0.01$, and *** = $P < 0.001$. Gastro = gastrocnemius muscle.

Normal activation of the NF-κB pathway in homozygous S467D mice

To further understand the importance of phosphorylation at p65 serine 467, we decided to generate an additional knock-in mouse model in which serine 467 is substituted by an aspartic acid ("phospho-mimetic"). A similar targeting strategy was used for the generation of the S467D allele (Supplemental Figure 5A). The mutant S467D allele was successfully engineered, confirmed by genotyping and sequence analysis (Supplemental Figures 5B-D). Homozygous S467D mice were obtained at the expected Mendelian frequency and looked overtly normal up to one year of age (Supplemental Figure 5E). Characterization of wild-type and *p65*$^{S467D/S467D}$ MEFs demonstrated that p65 protein levels are comparable in wild-type and homozygous knock-in cell lysates (Figure 5A). Next, we assessed whether the S467D mutation affects the upstream activation of the NF-κB pathway. Time course analysis after TNFα stimulation showed normal degradation and resynthesis of IκBα protein levels in homozygous knock-in MEFs (Figure 5B). In addition, we studied the kinetics of TNFα-induced phosphorylation of p65 at serine 467 and showed in wild-type MEFs that phosphorylation of serine 467 is an early event that disappeared after 30 minutes (Figure 5B). Of notice, the used antibody detected the mutated p65 protein in both unstimulated and stimulated S467D cells (Figure 5B). We observed similar kinetics of TNFα-stimulated p65 phosphorylation at serine 534 in both wild-type and *p65*$^{S467D/S467D}$ MEFs, although the total

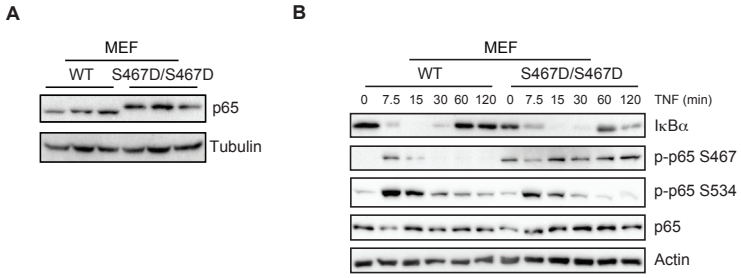

Figure 5. Characterization of *p65* S467D mutant MEFs. (A) Western blot analysis of p65 protein expression in wild-type and *p65*$^{S467D/S467D}$ MEFs. Tubulin was used as a loading control. **(B)** Immunoblot analysis of the degradation and resynthesis of IκBα proteins in whole cell extracts of MEFs after TNFα stimulation (10ng/ml). In addition, levels of phosphorylated p65 at serine 467 and serine 534 are shown. Actin was used as a loading control.

level of phosphorylated p65 at serine 534 was markedly reduced in homozygous knock-in MEFs (Figure 5B).

Increased activation of a subset of NF-κB target genes

To investigate whether the S467D mutation affects NF-κB-mediated gene expression in MEFs, we activated the NF-κB pathway and determined the expression of the same set of NF-κB target genes as we did for the S467A mutant. Except for *Icam1* and *Vcam1*, we observed no significant changes in TNFα-induced gene expression (Figure 6 and Supplemental Figure 6). The levels of *Icam1* and *Vcam1* mRNA were enhanced in *p65*$^{S467D/S467D}$ MEFs after 1.5 hours of stimulation (Figure 6). Altogether, these data suggest that the S467D mutation only affects the expression of a very small subset of NF-κB-mediated genes.

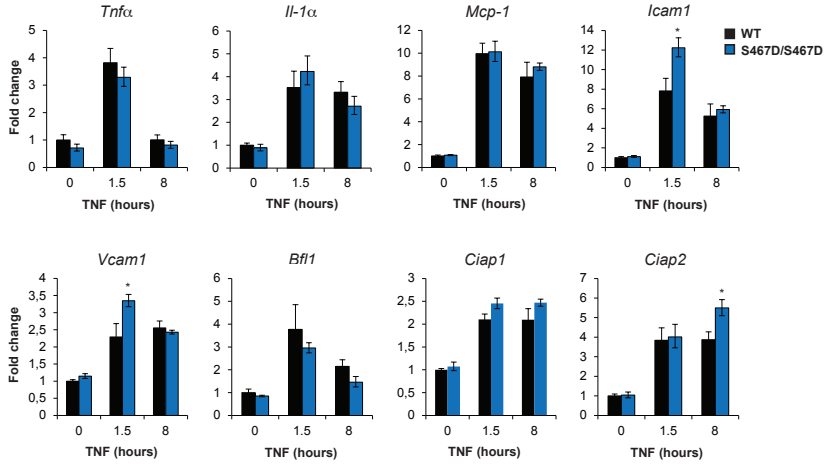

Figure 6. Enhanced activation of a subset of NF-κB target genes. Expression of pro-inflammatory cytokines, NF-κB target genes, and anti-apoptotic genes was determined by qRT-PCR in wild-type and *p65*$^{S467D/S467D}$ MEFs after TNFα stimulation (10ng/ml) at 0, 1,5 and 8 hours. Values represent 4 independent lines per genotype and represent average ± SEM, * = $P < 0.05$.

DISCUSSION

Post-translational modifications of the activating subunit of NF-κB p65 are essential in determining the duration and strength of nuclear NF-κB activity and its transcriptional output [8,9]. Phosphorylation of p65 can occur at various residues and results in either increased [10,12,17,24-28] or decreased [14-16,18,19,29-31] transcriptional activity depending on the stimuli, the phosphorylation sites and the target genes [8]. Serine 468 phosphorylation facilitates the binding of a multimeric ubiquitin ligase complex that mediates the ubiquitination and subsequent proteasomal-dependent removal of DNA-bound p65 on a subset of NF-κB regulated promoter sites [18,19]. Furthermore, this selective termination of transcription was confirmed in serine 468 mutant studies where absent phosphorylation resulted in gene-specific activation of NF-κB target genes [18,20]. To study the function of this specific phosphorylation site of p65 in more detail, we engineered two knock-in mouse models expressing a mutant p65, in which serine 467 is substituted with either an alanine (S467A) or an aspartic acid (S467D). We found that homozygous S467A mice have an impaired activation of *Icam1* and pro-inflammatory gene expression in various tissues upon TNFα stimulation, whereas expression of anti-apoptotic genes was unaltered. This suggests that phosphorylation at serine 467 of p65 is essential for the gene-specific activation of NF-κB-mediated expression *in vivo*. Additional studies are needed to explain the underlying mechanisms of this regulation, but one likely explanation would be the effect of the observed reduction in p65 protein levels in multiple tissues of $p65^{S467A/S467A}$ mice. Another option is that the S467A mutation increases the recruitment histone deacetylases that changes the epigenetic environment and leads to repression of a subset of genes, which was demonstrated for the S276A mutation [13]. Along this line, ChIP analysis on the *Cxcl2* promoter revealed enhanced levels of histone acetylation associated with decreased recruitment of histone deacetylase 1 in phospho-mimetic *p65* T435D mutants [28]. Furthermore, phosphorylation at serine 467 of p65 is necessary to induce a conformational change and absence of this conformational change might result in different protein-protein interactions [22].

In addition, we have revealed that homozygous S467A MEFs have lower p65 protein levels, reduced cell viability, and diminished TNFα-induced expression of various inflammatory cytokines, cell adhesion molecules and also anti-apoptotic genes. In contrast, $p65^{S467D/S467D}$ MEFs demonstrated an increased TNFα-inducible activation of *Icam1* and *Vcam1*, while expression of most NF-κB target genes was unaffected. These results were unexpected, as two previous studies in which they examined NF-κB target gene expression in $p65^{-/-}$ MEFs reconstituted with either human wild-type p65 or a non-phosphorylatable form of p65 (S468A) demonstrated increased expression of *Icam1* and *Vcam1* in the mutant MEFs [18,20]. They showed that mutant p65 protein had an increased stability and prolonged occupation on the *Icam1* promoter, suggesting that absent phosphorylation in S468A MEFs reduces ubiquitin/proteasomal degradation of p65 [18]. In contrast, in our studies we found that p65 protein levels were significantly diminished in the homozygous S467A MEFs, which was not due to impaired transcription. Possibly, the correction for input of total p65 protein for the reconstituted MEFs in this previous study may have actually resulted in an overexpression of the non-phosphorylatable form of p65. This could potentially explain the opposite effect on *Icam1* and *Vcam1* expression, but not the increased protein stability in S468A mutant MEFs [18,20].

Independent comparison of expression analysis in homozygous S467A and $p65^{+/-}$ MEFs excluded the possibility that reduced p65 protein levels alone are sufficient to explain

the impaired activation of NF-κB target genes in *p65*$^{S467A/S467A}$ MEFs. First, the transactivation of some NF-κB genes was unaffected in the homozygous S467A MEFs, whereas these are impaired in the *p65*$^{+/-}$ MEFs. Second, the levels of reduction in TNF-induced NF-κB-mediated gene expression were larger in *p65*$^{+/-}$ MEFs.

In contrast, the increased sensitivity in TNFα-induced cell death in homozygous S467A compared to *p65*$^{+/-}$ MEFs might be due to reduced p65 protein levels. Indirect comparison of anti-apoptotic gene expression revealed no differences between both genotypes, suggesting that another mechanism is responsible for the elevated cell death in the *p65*$^{S467A/S467A}$ MEFs. Perhaps, the p65 protein levels in *p65*$^{S467A/S467A}$ MEFs are below a certain threshold that causes increased TNFα-induced cell death, but additional experiments are necessary to determine the exact trigger of this reduced cell viability.

Collectively, our study supports the notion that serine 467 of murine *p65* plays a critical role in the gene-specific activation of NF-κB-mediated expression in both MEFs and mice. Interestingly, *in vivo* TNF injections in homozygous S467A mice showed reduced activation of inflammatory genes, while genes involved in apoptosis were unaffected. Therefore, it would be of great interest to further investigate the contribution of phosphorylated p65 at serine 467 in the progression of various inflammatory-related diseases.

MATERIAL AND METHODS

Generation of S467A and S467D mice

The *p65*^{S467A} allele was produced through recombineering as described before [32]. The genomic *p65* gene fragment spanning exons 8-11 was retrieved from BAC #bMQ-331N14 (129S7/SvEv ES Cell, Source BioScience) and transferred into pDTA.4B. Exon 11 was amplified with the following primers: forward (5'-AAGCTTTATGACCGCAGT-AGCTAG-3') and reverse (5'-AAGCTTTAGTGGAAGCCCTGT-CCTAG-3') and cloned into pZero (Invitrogen). Introduction of the S467A and S467D knock-in mutation into exon 11 was accomplished by site-directed mutagenesis using the following primers: forward (5'-GTTCACAGACCTGGCAGCTGTGGACAACTCAGA-3') and reverse (5'-TCTGAGTTGTCCACAGCTGCCAGGTCTGTGAAC-3') for S467A; forward (5'-GG-AGTGTTCACAGACCTGGCAGACGTCGACAACTCAGAGTTT CAGCAG-3') and reverse (5'- CTGCTGAAACTCTGAGTTGTCGACGTCTGCCA GGTCTGTGAACAC-TCC-'3) for S467D. The mutated exon 11 was amplified with the following primers: forward (5'-GGATCCAGCTTTATGACCGCAGTAGC-3'), reverse (5'-GCGGCCG-CTCTAGATAGTGGAAGCCCTGTCCTAG-3') and cloned into NotI- and BamHI-restricted pL452 vector harboring a loxP-neo-loxP cassette. Amplification of pL452_Exon11mut with primers containing 60 bp homology to RelA (forward: 5'- ACTGAGCCCGTGCTCCATGGTTCATCCTCTTCGCTGGCTTTGCAGC TGTAACATGGTGAGAGTACTAACAAAAGCTGGTACCGGGC-3' and reverse: 5'-CTCCTGG-AGCAAGAGGGATCTACGTTATGTGAAGGAACCCCACTCCTATT GAACCTTTTGGCGGCCGCTCTAGATAGTGGAAGC-3') was performed to enable the replacement of wild-type exon 11 by the mutated exon 11 preceding the loxP-neo-loxP cassette using recombineering [32]. The final PvuI-linearized targeting vector was electroporated into TL1 129Sv/E ES cells. After selection with G418 and expansion, transfectants were tested by Southern Blotting for the presence of the NEO;S467A or NEO;S467D cassette (Figure 1B and Supplementary Figure 5B). Chimeric mice were produced by microinjection of two independent ES cell targeted clones into C57BL/6 blastocysts. Chimeric males were crossed with C57BL/6 females and these chimeras successfully transmitted the targeted allele. Subsequently, *p65*$^{+/NEO;S467A}$ and *p65*$^{+/NEO;S467D}$ mice were crossed with *Hprt*-Cre recombinase mice to excise the NEO cassette. The following primers were used for PCR genotyping on ear DNA of mice used in our studies: forward (5'-GCGTGGCTCACAAGAGTGAC-3') and reverse (5'-ACCACCTGACCCAGCTC-TAC-3') for *p65*$^{+}$, *p65*^{S467A}, and *p65*^{S467D}; forward (5'-GCGTGGCTCACAAGAGT-GAC-3') and reverse (5'-GGCTGCTAAAGCGCATGCT-3') for *p65*$^{NEO;S467A}$ and *p65*$^{NEO;S467D}$; forward (5'-GCGGTCTGGCAGTAAAAACTA-TC-3') and reverse (5'-ACGAACCTGGTCGAAATCAGTG-3') for Cre. The presence of the S467A or S467D mutation was confirmed by sequencing of cDNA derived from livers of *p65*$^{+/+}$ and *p65*$^{S467A/S467A}$ mice or *p65*$^{+/+}$ and *p65*$^{S467D/S467D}$ mice using either the forward (5'-CTGTCTGCACCTGTTCCAAA-3') or reverse (5'-CTTAGGAGCTGATCTGACTC-3') primer (Figure 1D and Supplemental Figure 5D). All mice were on a mixed 129Sv/E x C57BL/6 genetic background and had ad libitum access to food. For *in vivo* activation of the NF-κB pathway, mice were injected with either 15 μg/kg mTNFα (R&D Systems, #410-MT) or PBS (control) via the orbital vein and sacrificed at the indicated times. Plasma and various tissues were harvested for further analysis. All animal-related studies were reviewed and approved by the Animal Care and Use Committee of the University of Groningen.

Generation and culture of MEFs

We intercrossed $p65^{+/S467A}$ or $p65^{+/S467D}$ mice to derive $p65^{+/+}$, $p65^{+/S467A}$, and $p65^{S467A/S467A}$ or $p65^{+/+}$, $p65^{+/S467D}$, and $p65^{S467D/S467D}$ MEFs, respectively, from individual 13.5-day-old fetuses. In short, the uterus was removed from a female that is at day 13.5 of her pregnancy and individual embryos were isolated. The embryonic membrane was removed and stored for genotyping. The head and abdominal organs were removed and the remaining embryo was minced thoroughly using a razor blade. The minced embryo was resuspended in 7 ml of trypsin/EDTA and incubated at 37°C/15 min, vortex every 2 min. MEFs were centrifuged at 1500rpm/5 min, resuspended in Dulbecco's modified Eagle's medium (Gibco, #31966-021; 10% FBS, Hyclone, #SV30160-03; 1x MEM non-essential amino acids, Gibco, #11140-035; Gentamycin 10µg/ml, Gibco, # 15710-049; 2-Mercaptoethanol 50µM, Gibco, #31350-010) and seeded in a T75 flask. Cells were frozen at low passages and we used low passage number for the described experiments. For gene expression analyses, 6 independent wild-type and homozygous knock-in lines were utilized. We seeded $3x10^5$ MEFs per 35-mm dish and activated the NF-κB pathway with 10 ng/ml TNFα. Cells were harvested in 1 ml QIAzol Lysis Reagent (Qiagen, #79306) at the indicated times.

Cell viability

For the cell viability assay, we used 3 independent wild-type and homozygous knock-in immortalized MEF lines. On day 0, $1x10^5$ MEFs per 35-mm dish were seeded for each condition. On day 2, normal medium was replaced by medium containing 0, 25, 50, 75 or 100 ng/ml mTNFα. After 24 hours, cells were harvested with trypsin and counted with Tryptan Blue. Relative cell numbers were calculated by setting the number of cells for the condition 0 ng/ml mTNFα at 100% for each MEF line.

Western blotting

Tissues were homogenized in potassium phosphate buffer (25mM kPi, 500mM EDTA, 1mM DTT) supplemented with phosphatase and protease inhibitors and boiled for 10 minutes. An amount of 30µg protein was loaded on Tris-HCl Polyacrylamide gel, samples were separated using SDS-PAGE and transferred to PVDF membrane (GE Healthcare, #RPN303F). Bands were visualized using ChemiDocTM XRS+ System (Bio-Rad Laboratories BV). Blots were probed with the following antibodies: rabbit anti-65 (C-20) (Santa Cruz Biotechnology Inc., #sc-372), mouse anti-β-Actin (Sigma-Aldrich BV, #A5441), rabbit anti-α-Tubulin (Cell Signaling, #2114), mouse anti-IκBα (L35A5) (Cell Signaling, #4814), rabbit anti-phospho-NF-κB p65 (Ser536) (93H1) (Cell Signaling, #3033), rabbit anti-phospho-NF-κB p65 (Ser468) (Cell Signaling, #3039), goat anti-rabbit IgG (H+L)-HRP Conjugate (Bio-Rad Laboratories BV, #170-6515), goat anti-mouse IgG (H+L)-HRP Conjugate (Bio-Rad Laboratories BV, #170-6516).

Quantitative real-time PCR

Murine tissues were homogenized in 1 ml QIAzol Lysis Reagent. Total RNA was isolated by chloroform extraction, precipitated with isopropanol, washed with ethanol and RNA pellets were dissolved in RNase/DNase-free water. Reverse transcription of 1µg RNA was performed using the Transcriptor Universal cDNA Master Kit (Roche, #05893151001) according to the protocol provided by the manufacturer. 20 ng cDNA was used for quantitative real-time PCR (qRT-PCR) using FastStart Universal SYBR Green Master (Rox) (Roche, #04913914001) and 7900HT Fast Real-Time PCR System (Applied Biosystems). The following PCR

program was used: 50°C/2 min, 95°C/10 min, 40 cycles of 95°C/15 sec and 60°C/1 min. Data was analyzed with the SDS 2.3 software. We used mouse *Cyclophilin A* as an internal control gene. The sequences of the used primers are listed in Supplemental Table 1.

Statistical analysis
Statistical analysis was performed using Prism (GraphPad Software) and the unpaired Student's t test.

ACKNOWLEDGEMENTS

We thank Paul Robbins for the generous gift of the $p65^{+/-}$ and $p65^{-/-}$ MEFs. This manuscript is supported by the Noaber Foundation, the Graduate School for Drug Exploration (GUIDE), and the University of Groningen.

REFERENCES

1. Hayden MS, West AP, Ghosh S (2006) NF-kappaB and the immune response. Oncogene 25: 6758–6780. doi:10.1038/sj.onc.1209943.
2. Hayden MS, Ghosh S (2008) Shared Principles in NF-κB Signaling. Cell 132: 344–362. doi:10.1016/j.cell.2008.01.020.
3. Hayden MS, Ghosh S (2012) NF-κB, the first quarter-century: remarkable progress and outstanding questions. Genes & Development 26: 203–234. doi:10.1101/gad.183434.111.
4. Tak PP, Firestein GS (2001) NF-kappaB: a key role in inflammatory diseases. J Clin Invest 107: 7–11. doi:10.1172/JCI11830.
5. Baker RG, Hayden MS, Ghosh S (2011) NF-κB, inflammation, and metabolic disease. Cell Metabolism 13: 11–22. doi:10.1016/j.cmet.2010.12.008.
6. Karin M, Cao Y, Greten FR, Li Z-W (2002) NF-kappaB in cancer: from innocent bystander to major culprit. Nat Rev Cancer 2: 301–310. doi:10.1038/nrc780.
7. Tilstra JS, Clauson CL, Niedernhofer LJ, Robbins PD (2011) NF-κB in Aging and Disease. Aging Dis 2: 449–465.
8. Huang B, Yang X-D, Lamb A, Chen L-F (2010) Posttranslational modifications of NF-kappaB: another layer of regulation for NF-kappaB signaling pathway. Cell Signal 22: 1282–1290. doi:10.1016/j.cellsig.2010.03.017.
9. Perkins ND (2006) Post-translational modifications regulating the activity and function of the nuclear factor kappa B pathway. Oncogene 25: 6717–6730. doi:10.1038/sj.onc.1209937.
10. Zhong H, Voll RE, Ghosh S (1998) Phosphorylation of NF-kappa B p65 by PKA stimulates transcriptional activity by promoting a novel bivalent interaction with the coactivator CBP/p300. Mol Cell 1: 661–671.
11. Zhong H, May MJ, Jimi E, Ghosh S (2002) The phosphorylation status of nuclear NF-kappa B determines its association with CBP/p300 or HDAC-1. Mol Cell 9: 625–636.
12. Dong J, Jimi E, Zeiss C, Hayden MS, Ghosh S (2010) Constitutively active NF-κB triggers systemic TNFα-dependent inflammation and localized TNFα-independent inflammatory disease. Genes & Development 24: 1709–1717. doi:10.1101/gad.1958410.
13. Dong J, Jimi E, Zhong H, Hayden MS, Ghosh S (2008) Repression of gene expression by unphosphorylated NF-κB p65 through epigenetic mechanisms. Genes & Development 22: 1159–1173. doi:10.1101/gad.1657408.
14. Msaki A, Sánchez AM, Koh LF, Barré B, Rocha S, et al. (2011) The role of RelA (p65) threonine 505 phosphorylation in the regulation of cell growth, survival, and migration. Mol Biol Cell 22: 3032–3040. doi:10.1091/mbc.E11-04-0280.
15. Buss H (2004) Phosphorylation of Serine 468 by GSK-3β Negatively Regulates Basal p65 NF-κB Activity. Journal of Biological Chemistry 279: 49571–49574. doi:10.1074/jbc.C400442200.
16. Schwabe RF (2005) IKKβ phosphorylates p65 at S468 in transactivaton domain 2. The FASEB Journal. doi:10.1096/fj.05-3736fje.
17. Mattioli I, Geng H, Sebald A, Hodel M, Bucher C, et al. (2006) Inducible Phosphorylation of NF-κB p65 at Serine 468 by T Cell Costimulation Is Mediated by IKK. Journal of Biological Chemistry 281: 6175–6183. doi:10.1074/jbc.M508045200.
18. Geng H, Wittwer T, Dittrich-Breiholz O, Kracht M, Schmitz ML (2009) Phosphorylation of NF-κB p65 at Ser468 controls its COMMD1-dependent ubiquitination and target gene-specific proteasomal elimination. EMBO Rep 10: 381–386. doi:10.1038/embor.2009.10.

19. Mao X, Gluck N, Li D, Maine GN, Li H, et al. (2009) GCN5 is a required cofactor for a ubiquitin ligase that targets NF-κB/RelA. Genes & Development 23: 849–861. doi:10.1101/gad.1748409.
20. Moreno R, Sobotzik JM, Schultz C, Schmitz ML (2010) Specification of the NF-κB transcriptional response by p65 phosphorylation and TNF-induced nuclear translocation of IKK. Nucleic Acids Research 38: 6029–6044. doi:10.1093/nar/gkq439.
21. Tang S-HE, Silva FJ, Tsark WMK, Mann JR (2002) A Cre/loxP-deleter transgenic line in mouse strain 129S1/SvImJ. Genesis 32: 199–202.
22. Milanovic M, Kracht M, Schmitz ML (2014) The cytokine-induced conformational switch of nuclear factor κB p65 is mediated by p65 phosphorylation. Biochem J 457: 401–413. doi:10.1042/BJ20130780.
23. Geisler F, Algül H, Paxian S, Schmid RM (2007) Genetic inactivation of RelA/p65 sensitizes adult mouse hepatocytes to TNF-induced apoptosis in vivo and in vitro. Gastroenterology 132: 2489–2503. doi:10.1053/j.gastro.2007.03.033.
24. Anrather J, Racchumi G, Iadecola C (2005) cis-Acting, element-specific transcriptional activity of differentially phosphorylated nuclear factor-kappa B. J Biol Chem 280: 244–252. doi:10.1074/jbc.M409344200.
25. Duran A, Diaz-Meco MT, Moscat J (2003) Essential role of RelA Ser311 phosphorylation by zetaPKC in NF-kappaB transcriptional activation. EMBO J 22: 3910–3918. doi:10.1093/emboj/cdg370.
26. Wang D, Westerheide SD, Hanson JL, Baldwin AS (2000) Tumor necrosis factor alpha-induced phosphorylation of RelA/p65 on Ser529 is controlled by casein kinase II. J Biol Chem 275: 32592–32597. doi:10.1074/jbc.M001358200.
27. Buss H, Dörrie A, Schmitz ML, Hoffmann E, Resch K, et al. (2004) Constitutive and interleukin-1-inducible phosphorylation of p65 NF-{kappa}B at serine 536 is mediated by multiple protein kinases including I{kappa}B kinase (IKK)-{alpha}, IKK{beta}, IKK{epsilon}, TRAF family member-associated (TANK)-binding kinase 1 (TBK1), and an unknown kinase and couples p65 to TATA-binding protein-associated factor II31-mediated interleukin-8 transcription. J Biol Chem 279: 55633–55643. doi:10.1074/jbc.M409825200.
28. O'Shea JM, Perkins ND (2010) Thr435 phosphorylation regulates RelA (p65) NF-kappaB subunit transactivation. Biochem J 426: 345–354. doi:10.1042/BJ20091630.
29. Rocha S, Garrett MD, Campbell KJ, Schumm K, Perkins ND (2005) Regulation of NF-kappaB and p53 through activation of ATR and Chk1 by the ARF tumour suppressor. EMBO J 24: 1157–1169. doi:10.1038/sj.emboj.7600608.
30. Campbell KJ, Witty JM, Rocha S, Perkins ND (2006) Cisplatin mimics ARF tumor suppressor regulation of RelA (p65) nuclear factor-kappaB transactivation. Cancer Res 66: 929–935. doi:10.1158/0008-5472.CAN-05-2234.
31. Lawrence T, Bebien M, Liu GY, Nizet V, Karin M (2005) IKKalpha limits macrophage NF-kappaB activation and contributes to the resolution of inflammation. Nature 434: 1138–1143. doi:10.1038/nature03491.
32. Malureanu LA (2011) Targeting vector construction through recombineering. Methods Mol Biol 693: 181–203. doi:10.1007/978-1-60761-974-1_11.

SUPPLEMENTAL FIGURES

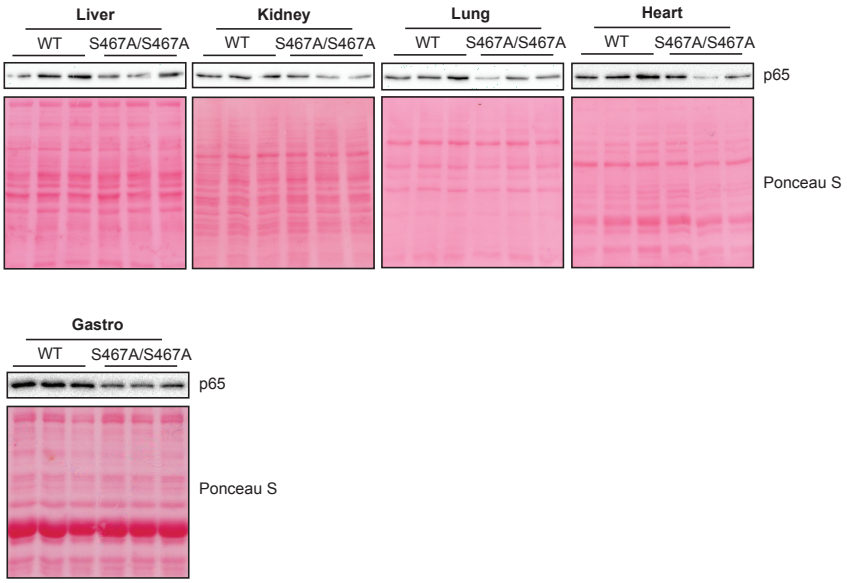

Supplemental Figure 1. Diminished total p65 protein levels in *p65*$^{S467A/S467A}$ mice. Western blot analysis of p65 protein levels in various tissues of 3-month-old male wild-type and homozygous knock-in mice. Ponceau S staining was used as a loading control. Gastro = gastrocnemius muscle.

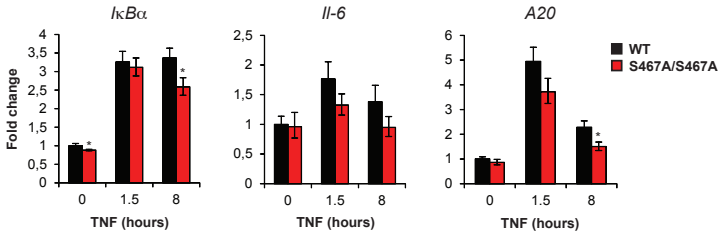

Supplemental Figure 2. Transactivation of additional NF-κB target genes was not markedly impaired in S467A MEFs. qRT-PCR analysis was used to determine mRNA expression of *IκBα*, *Il6* and *A20* at 0, 1,5 and 8 hours following TNFα stimulation (10ng/ml). We used 6 independent wild-type and S467A MEF lines. All values represent average ± SEM, * = $P < 0.05$.

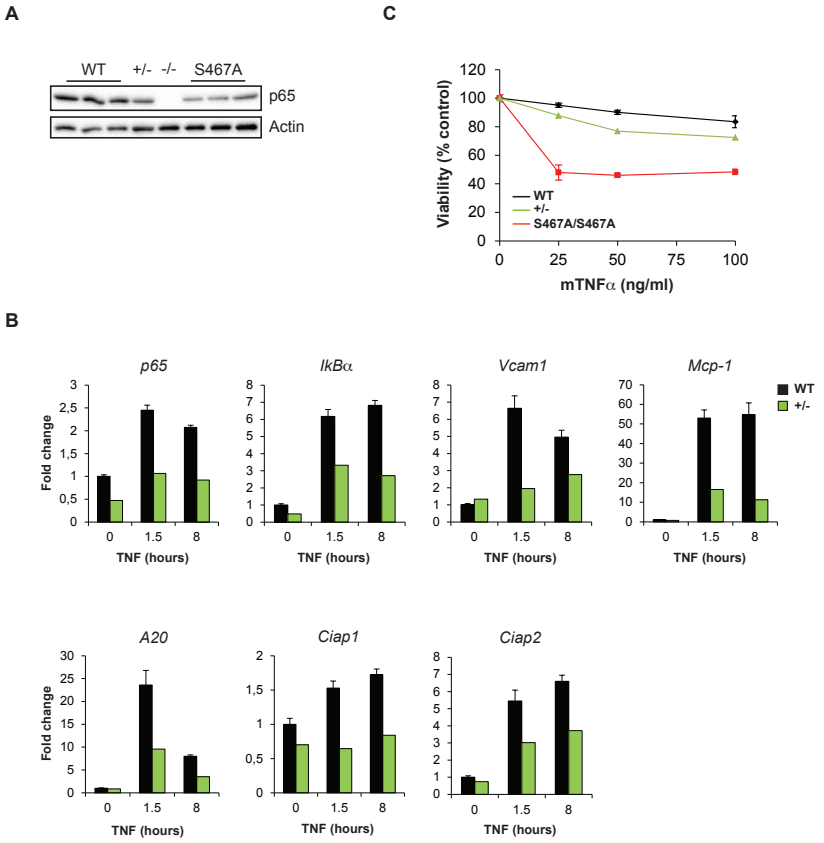

Supplemental Figure 3. Haplo-insufficiency of *p65* results in compromised NF-κB-mediated transcription. **(A)** Western blot analysis of p65 protein levels in $p65^{+/+}$, $p65^{+/-}$, $p65^{-/-}$ and $p65^{S467A/S467A}$ MEFs. **(B)** Relative mRNA expression of NF-κB target genes in wild-type and $p65^{+/-}$ MEFs at 0, 1,5 and 8 hours after TNFα stimulation. **(C)** Cell viability was determined in $p65^{+/+}$, $p65^{+/-}$, and homozygous S467A MEFs following 24 hours exposure to various concentrations of TNFα.

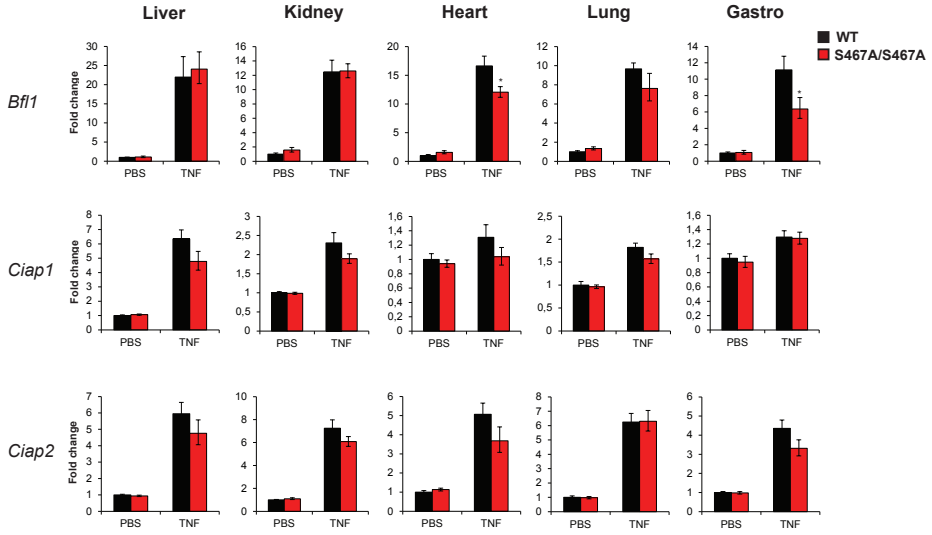

Supplemental Figure 4. Homozygous S467A mice demonstrate normal activation of anti-apoptotic genes. Relative mRNA expression of anti-apoptotic genes was assessed by qRT-PCR in various tissues at 1 hour after injection with either PBS or TNFα (15μg/kg). PBS, n = 7 male mice per genotype; TNFα, n = 6 male mice per genotype. All values represent average ± SEM, * = $P < 0.05$.

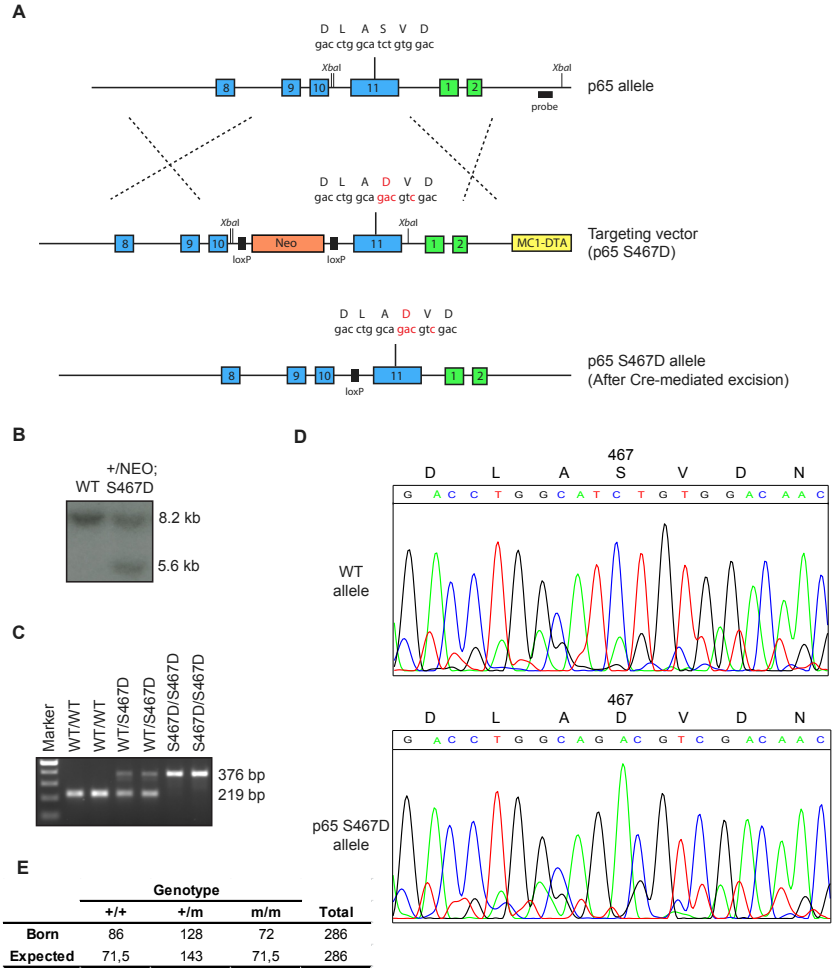

	Genotype			
	+/+	+/m	m/m	Total
Born	86	128	72	286
Expected	71,5	143	71,5	286

Supplemental Figure 5. Generation of *p65* S467D knock-in mice. (A) Gene targeting strategy to generate $p65^{S467D/S467D}$ mice. Indicated are the genomic mouse p65 locus spanning exon 8-11 of *p65* and exon 1-2 of *Sipa1* (top); the targeting vector with the S467D mutation in exon 11 (red), loxP sites (black boxes); the p65 S467D locus after targeted recombination and crossing with *Hprt*-Cre recombinase mice to remove the NEO cassette and produce $p65^{+/S467D}$ mice. **(B)** Southern blot of *Xba*I digested genomic DNA from two ES cell clones and probed with DNA fragment showing the 8.2 kb and 5.6 kb fragments representing the wild-type and $p65^{NEO;S467D}$ alleles, respectively. **(C)** PCR genotyping of DNA extracted from two wild-type, two $p65^{+/S467D}$ and two $p65^{S467D/S467D}$ mice. **(D)** Sequencing of p65 cDNA obtained by RT-PCR from livers of wild-type and $p65^{S467D/S467D}$ mice. **(E)** Genotype analysis of offspring derived from breeding S467D heterozygous parents. The expected Mendelian frequency is indicated at the bottom.

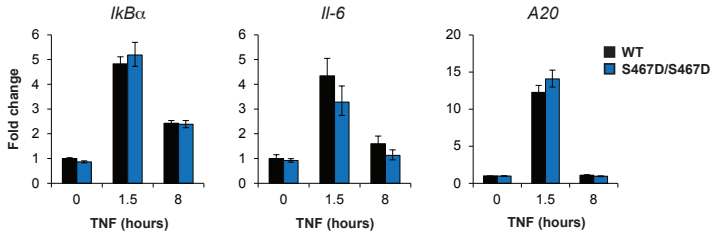

Supplemental Figure 6. NF-κB-mediated gene expression is unaffected in *p65* S467D MEFs. Expression of the NF-κB target genes: *IκBα*, *Il6* and *A20* was determined by qRT-PCR at 0, 1,5 and 8 hours after TNFα stimulation (10ng/ml). We used 4 independent wild-type and homozygous knock-in MEF lines. All values represent average ± SEM.

Supplemental Table 1. qRT-PCR primer sequences.

Gene	Forward 5' -> 3'	Reverse 5' -> 3'
p65	ACCGCTGCATCCACAGTT	GGATGCGCTGACTGATAGC
Cyclophilin A	TTCCTCCTTTCACAGAATTATTCCA	CCGCCAGTGCCATTATGG
Tnfα	GTAGCCCACGTCGTAGCAAAC	AGTTGGTTGTCTTTGAGATCCATG
Il-1α	AACCAAACTATATATCAGGATGTG	ACGGGCTGGTCTTCTCCTTG
Mcp-1	GCTGGAGAGCTACAAGAGGATCA	ACAGACCTCTCTCTTGAGCTTGGT
Icam1	ACTGCACGTGCTGTATGGTC	CTGCAGGTCATCTTAGGAGATG
Vcam1	AGTTGGGGATTCGGTTGTTCT	CCCCTCATTCCTTACCACCC
Bfl1	AGATTGCCCTGGATGTATGTG	CTCTCTGGTCCGTAGTGTTAC
Ciap1	GACCGTCAATGATATTGTCTCAG	TGGCCTCAAGAAGATTATCCAG
Ciap2	AGGAGGAGGAGTCAGATGATC	CTGAATGAGGTTGCTGCAGTG
IκBα	TGGAAGTCATTGGTCAGGTGAA	CAGAAGTGCCTCAGCAATTCCT
Il-6	CTGCAAGAGACTTCCATCCAGTT	AGGGAAGGCCGTGGTTGT
A20	GCTCTGAAAACCAATGGTGATG	CCGAGTGTCTGTCTCCTTAAG